Quantitative Time-of-Flight Head Magnetic Resonance Angiography of Cerebrovascular Disease

Ioannis Koktzoglou, PhD,[1,2*] Onural Ozturk, MD,[1,3] Matthew T. Walker, MD,[1,2] William J. Ankenbrandt, MD,[1,2] Archie L. Ong, MD,[2,4,†] William J. Ares, MD,[2,5] Fulvio R. Gil, MD,[2,4] Zachary B. Bulwa, MD,[2,4] and Robert R. Edelman, MD[1,3]

Background: Standard Cartesian time-of-flight (TOF) head magnetic resonance angiography (MRA) is routinely used to evaluate the intracranial arteries, but does not provide quantitative hemodynamic information that is useful for patient risk stratification as well as for monitoring treatment and tracking changes in blood flow over time. Quantitative TOF (qTOF) MRA represents a new and efficient method for simultaneous evaluating the intracranial arteries and quantifying blood flow velocity, but it has not yet been evaluated in patients with cerebrovascular disease.
Purpose: To evaluate qTOF for simultaneously evaluating the intracranial arteries and quantifying intracranial blood flow velocity in patients with cerebrovascular disease, without the need for a phase contrast (PC) scan.
Study Type: Prospective.
Subjects: Twenty-four patients (18 female, 6 male) with cerebrovascular disease.
Field Strength/Sequences: Head MRA at 3 T using gradient-echo 3D qTOF, standard Cartesian TOF, and PC protocols.
Assessment: Three independent readers assessed arterial image quality using a 4-point scale (1: non-diagnostic, 4: excellent) and artifact presence. Total and component flow velocities obtained with qTOF and PC were measured.
Statistical Tests: Wilcoxon signed-rank tests, Gwet's AC2, intraclass correlation coefficients (ICC) for absolute agreement, Bland–Altman analyses, tests of equal proportions. *P* values <0.05 were considered statistically significant.
Results: Averaged across readers and compared to standard Cartesian TOF, qTOF significantly improved overall arterial image quality (3.8 ± 0.2 vs. 3.6 ± 0.5), image quality at locations of pathology (3.7 ± 0.5 vs. 3.4 ± 0.7), and increased the proportion of evaluations rated without artifacts (63.9% [46/72] vs. 37.5% [27/72]). qTOF significantly agreed with PC for total flow velocity (ICC = 0.71) and component flow velocity (ICC = 0.89).
Data Conclusion: qTOF angiography of the head matched or improved upon the image quality of standard Cartesian TOF, reduced image artifacts, and provided quantitative hemodynamic data, without the need for a PC scan.
Evidence Level: 2
Technical Efficacy: Stage 2

J. MAGN. RESON. IMAGING 2024.

Cerebrovascular disease is an arterial disease of the head and neck, and is a common cause of mortality and morbidity that afflicts many millions of people annually worldwide.[1,2] Cerebrovascular disease is often imaged using the non-invasive cross-sectional imaging modalities of computed tomography and magnetic resonance imaging. Large arterial imaging with these modalities is typically performed using computed tomography angiography and magnetic resonance angiography (MRA). MRA, performed using the widely available time-of-flight (TOF) technique, provides relatively high

View this article online at wileyonlinelibrary.com. DOI: 10.1002/jmri.29395

Received Jan 22, 2024, Accepted for publication Mar 29, 2024.

*Address reprint requests to: I.K., Walgreen Jr. Building, G507, 2650 Ridge Ave., Evanston, IL 60201, USA.
E-mail: ikoktzoglou@gmail.com

From the [1]Department of Radiology, Endeavor Health, Evanston, Illinois, USA; [2]University of Chicago Pritzker School of Medicine, Chicago, Illinois, USA; [3]Northwestern University Feinberg School of Medicine, Chicago, Illinois, USA; [4]Department of Neurology, Endeavor Health, Evanston, Illinois, USA; [5]Department of Neurosurgery, Endeavor Health, Evanston, Illinois, USA

[†]**Present address:** Department of Neurology, Northwestern Lake Forest Hospital, Lake Forest, Illinois, USA

spatial resolution and avoids the use of contrast agents and ionizing radiation.[3] However, TOF MRA does not provide quantitative hemodynamic information,[4] which is predictive of stroke[5,6] and enables quantitative monitoring of cerebral blood flow and the impact of treatment.[7,8]

Quantitative hemodynamic data within the intracranial arteries can be obtained with phase contrast (PC) MRA.[4,9] However, PC is not routinely included in most clinical head MRA protocols due to lengthy additional acquisition times, lower spatial resolution and lesional sensitivity than TOF, and because vessel depiction depends on patient blood velocity and the applied PC velocity encoding sensitivity.[10–14] Recent work has suggested that quantitative hemodynamic information can be added to head MRA using a quantitative variant of TOF referred to as "quantitative TOF" (qTOF).[15,16] Analogous to a high-speed camera, the qTOF method collects two or more echo time images (TEs) (i.e., "snapshots") that are used to quantify intracranial arterial flow velocity based on small flow-dependent displacements across acquired TEs. The qTOF method also provides the potential for improved structural display of the intracranial arteries through reduction of flow-related displacement artifacts.[15] Nonetheless, initial studies with qTOF have only been done in healthy human subjects. Consequently, it remains unclear how qTOF performs for both structural and hemodynamic evaluation of cerebral arteries in patients with cerebrovascular disease.

The purpose of this study was to evaluate how qTOF performs in patients with cerebrovascular disease.

Materials and Methods

This study was approved by our institutional review board and all participants provided written informed consent.

Human Subjects

Twenty-five adults with cerebrovascular disease participated in the study. One case was excluded due to an MRI system technical issue and 24 cases (mean age 54 ± 15 years, 18 female/6 male) were included in the final analysis. Indications for imaging included intracranial arterial stenosis or atherosclerosis (N = 14), aneurysm (N = 7; 5 treated, 2 untreated), extracranial arterial stenosis or occlusion (N = 2), and vertebral artery dissection (N = 1). Of these patients, eight had a history of ischemic stroke, seven had a history of transient ischemic attack, and one had a history of aneurysmal subarachnoid hemorrhage. Five patients had intracranial aneurysms previously treated with flow diverters or coils.

Imaging Parameters

MRI was done on a 3 Tesla system (Skyra^{fit}, Siemens Healthineers, Erlangen, Germany) equipped with a 16-channel head coil. MRI was done using the 3D gradient-echo protocols of TOF, prototype qTOF, and PC. Typical imaging parameters are listed in Table 1

TABLE 1. Imaging Parameters

Parameter	TOF	qTOF	PC
Acquisition type	3D cartesian	3D stack-of-stars	3D cartesian
TR (msec)	21.0	21.0	39.9
TE (msec)	3.4	3.4, 7.8, 15.0	5.9
Flip angle (°)	15	15	10
Field of view (mm)	205 × 221	258 × 258	218 × 218
Matrix	356 × 384	448 × 448	256 × 256
Spatial resolution (mm^3)	0.58 × 0.58 × 1.00 (0.29 × 0.29 × 0.50)	0.58 × 0.58 × 1.00 (0.29 × 0.29 × 0.50)	0.85 × 0.85 × 1.30 (0.43 × 0.43 × 0.65)
GRAPPA factor	2	–	2
Slices	104	104	80
Slabs	3	3	1
Ramped RF pulses	Yes	Yes	No
Bandwidth (Hz/px)	186	587	444
VENC	–	–	60–90 cm/s
Scan time	4 min 3 s	4 min 3 s	4 min 4 s

Spatial resolution given in form: acquired (interpolated). GRAPPA = generalized autocalibrating partial parallel acquisition; RF = radiofrequency; PC = phase contrast; TOF = time-of-flight; qTOF = quantitative time-of-flight; VENC = velocity encoding sensitivity.

and for qTOF and TOF were as follows: spatial resolution of $0.58 \times 0.58 \times 1.0$ mm^3 (interpolated to $0.29 \times 0.29 \times 0.5$ mm^3), flow compensation, scan time of 4 minutes and 3 seconds, flip angles of 15°, TE of 3.4 msec. Imaging parameters for PC were: spatial resolution of $0.85 \times 0.85 \times 1.3$ mm^3 (interpolated to $0.43 \times 0.43 \times 0.65$ mm^3), scan time of 4 minutes and 4 seconds, flip angle of 10°, TE of 5.4 msec. PC was acquired with baseline velocity encoding sensitivities of 60–75 cm/s and was reacquired with a larger velocity encoding sensitivity (typically 90 cm/s) in cases of velocity aliasing. For qTOF, a second flow-compensated TE of 7.8 msec was used for hemodynamic quantitation, whereas an additionally acquired dark-blood TE of 15.0 msec was filtered and subtracted from the shortest first TE to improve arterial-to-background contrast and arterial conspicuity.

Image Review: Qualitative Scoring and Pathology Detection

TOF and qTOF were evaluated independently by three readers: two fellowship-trained subspecialty-certified neuroradiologists (MW and WA; readers 1 and 2) with 25 and 28 years of experience, and one fellowship-trained radiologist (OO; reader 3) with 5 years of experience. Readers were blinded to scan type and patient clinical history. qTOF source images were reviewed first, followed by at least a four-week hiatus, after which TOF source images were reviewed. TOF source images were flipped horizontally to further minimize recall bias. Images were reviewed using a professional digital imaging and communications in medicine (DICOM) viewer (InteleViewer, version 5-3-1-P333, Intelerad Medical Systems, Montreal, Canada).

For each imaging volume, each reader scored overall large vessel image quality (covering the internal carotid arteries, basilar artery, and first and second order segments of the middle, posterior, and anterior cerebral arteries), overall small vessel image quality (covering the third and fourth order branches of the middle cerebral arteries), and the presence of artifacts affecting arterial evaluation. Image quality was rated using a 4-point scale: 1—"non-diagnostic," image quality inadequate for diagnosis; 2—"fair," image quality marginally acceptable for diagnosis; 3—"good," image quality adequate for confident diagnosis; and 4—"excellent," image quality providing highly confident diagnosis. Large and small vessel image quality scores were averaged to generate an "overall image quality" score.

Image artifacts were assessed using a 4-point scale: 1—"severe" artifact affecting diagnosis; 2—"moderate" artifact not affecting diagnosis; 3—"minor" artifact not affecting diagnosis; and 4—"no artifact" affecting diagnosis. If artifacts were present, readers attributed them to either "ghosting," "motion," "flow," or "susceptibility"; multiple artifact types could be selected for a single data set. "Motion," "ghosting," and "flow" artifacts were retrospectively aggregated into a single artifact category "motion/flow."

Arterial pathology at locations without metallic flow diverters or coils were evaluated for image quality (using the aforementioned 4-point scale). Stenoses were graded visually using the following scale: 1—normal patency or <50% stenosis; 2—50%–69% stenosis; 3—70%–99% stenosis; 4—occlusion; and 5—non-diagnostic/indeterminate. Aneurysm size was measured at the location of maximal dome diameter.

After initial reads were completed in a blinded manner, retrospective unblinded side-by-side review of qTOF and TOF was done independently by each reader at locations of vascular pathology prospectively found (according to that reader) by one method and not the other. Readers evaluated whether there was retrospective agreement of noted pathology.

Quantitative Hemodynamic Evaluation

3D PC data were spatially interpolated and rigidly registered to the higher spatial resolution qTOF volumes. Arterial segmentation for qTOF and PC was done using region growing to generate masks for both volumes. qTOF data were analyzed to quantify intracranial arterial flow velocity using in-house software[15] incorporating 16 rotated planes of directional analysis.[16]

qTOF arterial mask data were skeletonized to identify vessel centerline locations. Component and total flow velocity measurements were obtained every 3 mm along all vessel centerline locations within 27 mm^3-sized cubes containing at least 0.5 mm^3 of arterial mask overlap between qTOF and PC; component and total velocities within these small regions were averaged. Local region growing (seeded at qTOF centerline locations and constrained to these small cubic regions) was done to ensure arterial signal compared originated from the same vessel/location. Locations of velocity aliasing on PC—identified if the intraregional velocity span exceeded the velocity encoding sensitivity—prompted use of PC data acquired with a larger velocity encoding if available; if such PC data were not available, measurements at these locations were excluded from analysis. Typical vessel regions analyzed and included in the final analysis spanned the bilateral distal internal carotid arteries, M1, M2, and M3 segments of the middle cerebral arteries, P1, P2, and P3 segments of the posterior cerebral arteries, A1 and A2 segments of the anterior cerebral arteries, and the distal basilar artery.

Mean total flow velocities in the most proximal downstream intracranial arteries were measured and compared to contralateral arteries in subjects with a history of unilateral stroke, ≥50% stenosis, or flow diverter in-stent stenosis or arterial bridging.

Statistical Analysis

Due to non-normality, image quality scores and stenosis grades obtained with qTOF and TOF were compared using Wilcoxon signed-rank tests. Inter-reader agreement was assessed using quadratically weighted Gwet's AC2 statistic[17]; agreement values of 0.01–0.20, 0.21–0.40; 0.41–0.60, 0.61–0.80, and 0.81–0.99 were considered as "slight," "fair," "moderate," "substantial," and "almost perfect."[18] Hemodynamic data obtained with PC and qTOF were compared using linear regression analysis for computation of Pearson correlation coefficient (r), two-way single measures intraclass correlation coefficient (ICC) for absolute agreement, and Bland Altman analysis. Pearson r values of ≤0.30, 0.31–0.69, and ≥0.70 were interpreted to indicate "weak," "moderate," and "strong" correlation, respectively.[19] ICC values of <0.40, 0.40–0.59, 0.60–0.74, and ≥0.75 were considered as "poor," "fair," "good," and "excellent" agreement, respectively.[20] Artifact incidence data were compared using tests of equal proportions. Data were presented as mean ± SD unless otherwise noted. P values <0.05 were considered statistically significant. Analyses were done using R software (version 4.2.2, The R Foundation for Statistical Computing, Vienna, Austria).

Results

Image Quality and Pathology Detection

Figures 1 and 2 show examples of qTOF and TOF data acquired in patients with arterial stenosis and aneurysm, respectively. Figure 3 shows examples of artifacts observed in the study.

IMAGE QUALITY. Large arterial, small arterial, and overall image quality scores are presented in Table 2. On average across readers, large arterial image quality was generally rated as excellent and significantly differed between qTOF and TOF (3.8 ± 0.3 vs. 3.5 ± 0.5). Respective small arterial image quality scores significantly differed and were 3.8 ± 0.2 and 3.6 ± 0.5. Averaged across readers, overall image quality scores significantly differed and were 3.8 ± 0.2 for qTOF and 3.6 ± 0.5 for TOF. Reader 3 significantly preferred qTOF for large arterial image quality, small arterial image quality, and overall image quality, whereas no significant differences for these measures were observed for readers 1 and 2. For qTOF, inter-reader agreement was significant for large arterial image quality (AC2 = 0.87, 95% confidence interval [CI]: 0.73–1.00) and small arterial image quality (AC2 = 0.89, 95% CI: 0.79–0.99). For TOF, inter-reader agreement was significant for both large (AC2 = 0.77, 95% CI: 0.62–0.92) and small arterial image quality (AC2 = 0.80, 95% CI: 0.70–0.90).

Image artifact scoring data are summarized in Table 3. Averaged across readers, respective artifact scores obtained with qTOF and TOF were 3.5 ± 0.6 and 3.2 ± 0.6 ($P = 0.23$), corresponding to "mild" or "no" artifact. Image

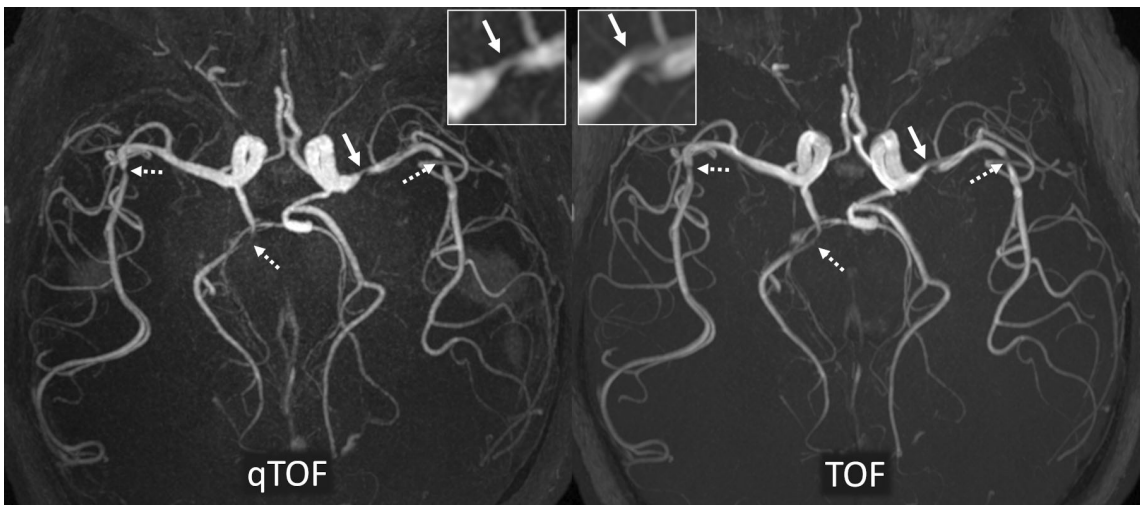

FIGURE 1: Maximum intensity projections of quantitative time-of-flight (qTOF) and standard Cartesian time-of-flight (TOF) magnetic resonance angiography in a patient with a severe stenosis of the left M1 segment (solid arrows) and other intracranial stenoses (dashed arrows). Insets show magnified views of the left M1 stenosis.

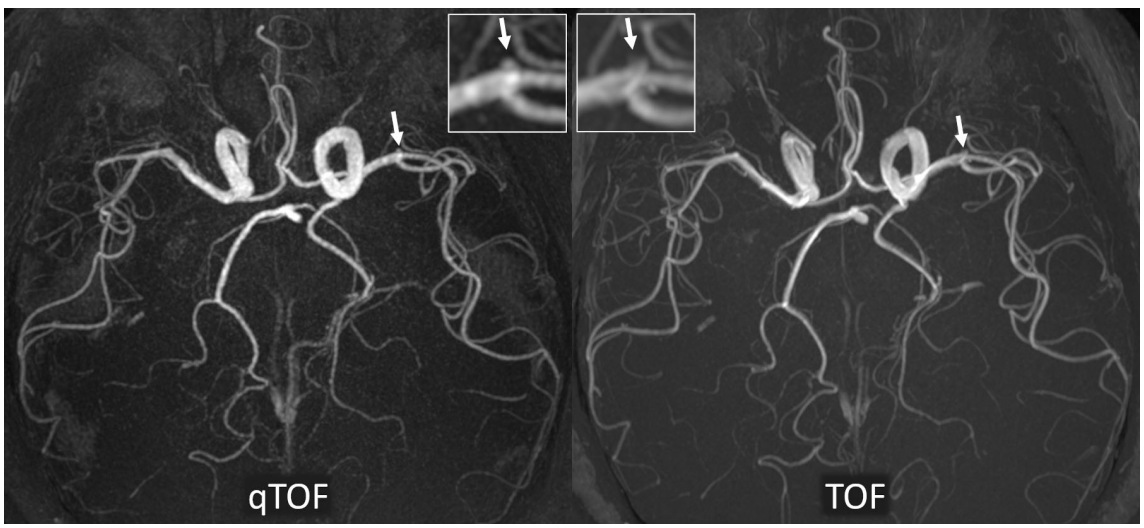

FIGURE 2: Maximum intensity projections of quantitative time-of-flight (qTOF) and standard Cartesian time-of-flight (TOF) magnetic resonance angiography in a patient with a small aneurysm (arrows) at the left MCA bifurcation. Insets show magnified views of the aneurysm.

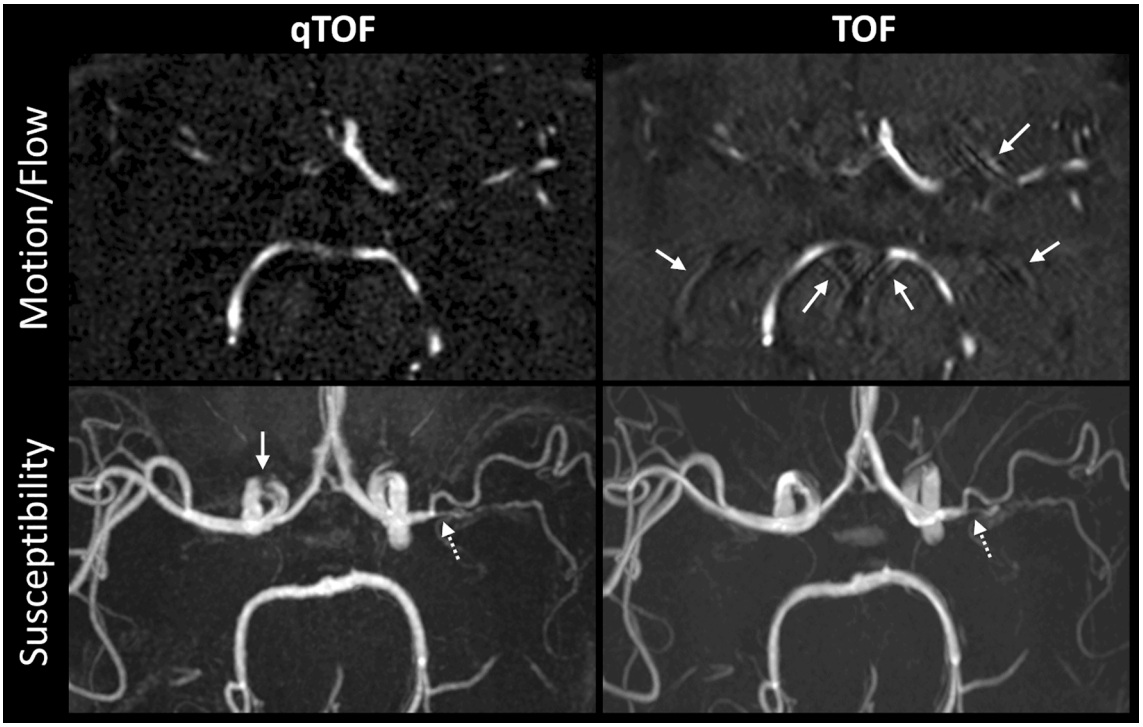

FIGURE 3: Examples of image artifacts encountered. Top row: source images showing ghost artifacts (arrows) from arterial pulsation (attributed to the "motion/flow" category) seen on standard Cartesian time-of-flight (TOF) magnetic resonance angiography. Bottom row: maximum intensity projection images showing magnetic susceptibility artifact seen on quantitative time-of-flight (qTOF) (solid arrow) in a subject with severe left M2 stenosis (dashed arrows).

TABLE 2. Image Quality Data

	Large Artery			Small Artery			Overall		
Reader	**qTOF**	**TOF**	***P*-Value***	**qTOF**	**TOF**	***P*-Value***	**qTOF**	**TOF**	***P*-Value***
1	3.9 ± 0.4	3.6 ± 0.6	0.197	3.9 ± 0.4	3.8 ± 0.7	0.571	3.9 ± 0.4	3.7 ± 0.6	0.205
2	3.7 ± 0.6	3.5 ± 0.7	0.482	3.7 ± 0.5	3.8 ± 0.6	0.608	3.7 ± 0.5	3.6 ± 0.6	1.00
3	4.0 ± 0.2	3.5 ± 0.7	**0.006**	4.0 ± 0.0	3.3 ± 0.6	**<0.001**	4.0 ± 0.1	3.4 ± 0.5	**<0.001**
Reader average	3.8 ± 0.3	3.5 ± 0.5	**0.014**	3.8 ± 0.2	3.6 ± 0.5	**0.034**	3.8 ± 0.2	3.6 ± 0.5	**0.007**

Presented as mean ± SD; higher numbers are better. qTOF = quantitative time-of-flight; TOF = time-of-flight.
*Wilcoxon signed-rank tests; bold text indicates statistical significance ($P < 0.05$).

artifact incidence data are presented in Table 4. In 72 ratings made by the readers (3 readers × 24 cases), qTOF and TOF were rated without artifact in 63.9% (46/72) and 37.5% (27/72) of cases, which significantly differed. No differences between qTOF and TOF were found for susceptibility artifacts (34.7% vs. 22.2%; $P = 0.14$), whereas motion/flow artifacts were significantly less prevalent in qTOF than in TOF (4.2% vs. 43.1%).

EVALUATION OF PATHOLOGY. The total number of arterial pathology detected by readers 1, 2, and 3 upon review of qTOF was 35, 26, and 40; respective numbers identified with TOF were 25, 33, and 28. The number of stenoses identified with qTOF (TOF) was 31 (22), 24 (31), and 36 (24) for readers 1, 2, and 3, respectively. The number of aneurysms identified with qTOF (TOF) was 4 (3), 2 (2), and 4 (4) for readers 1, 2, and 3, respectively.

Averaged across readers, image quality at locations of pathology significantly differed between qTOF and TOF (3.7 ± 0.5 vs. 3.4 ± 0.7). No significant differences between qTOF and TOF were found for stenosis grades (2.8 ± 0.7 vs. 2.6 ± 0.9, respectively; $P = 0.16$). Aneurysm sizes

measured by qTOF and TOF were 2.1 ± 1.1 mm and 2.4 ± 0.6 mm, respectively. At locations of pathology identified on both sequences and by the same reader, no differences in image quality scores between qTOF and TOF were found for reader 1 (N = 20, 3.7 ± 0.7 vs. 3.7 ± 0.7; $P = 0.83$) and reader 2 (N = 23, 3.5 ± 0.7 vs. 3.3 ± 0.6; $P = 0.30$), whereas image quality significantly differed for reader 3 (N = 22, 3.9 ± 0.4 vs. 3.2 ± 0.7). In these locations, no differences in stenosis grades were detected for reader 1 (N = 17, 3.0 ± 0.9 vs. 2.7 ± 1.2; $P = 0.12$), reader 2 (N = 21, 2.6 ± 0.6 vs. 2.5 ± 0.8; $P = 0.45$), and reader 3 (N = 19, 2.9 ± 0.9 vs. 2.8 ± 1.1; $P = 0.84$). Inter-reader agreement for lesion-specific image quality scores was significant for qTOF (AC2 = 0.78, 95% CI: 0.53–1.00) and TOF (AC2 = 0.71, 95% CI: 0.61–0.80). Inter-reader agreement for stenosis grading was significant for qTOF (N = 16, AC2 = 0.68, 95% CI: 0.43–0.94) and TOF (N = 11, AC2 = 0.82, 95% CI: 0.64–0.99).

Retrospective side-by-side reviews of qTOF and TOF at locations of pathology noted by one method and not the other found agreement between methods in all but four instances across the three readers. In these four instances, pathology was deemed by readers to be at most mild or too subtle to be called on standard TOF.

TABLE 3. Artifact Scoring Data

Reader	qTOF	TOF	*P*-Value*
1	3.7 ± 0.6	3.3 ± 0.8	0.081
2	3.3 ± 1.0	3.3 ± 0.7	0.976
3	3.4 ± 0.6	3.1 ± 0.8	0.166
Reader average	3.5 ± 0.6	3.2 ± 0.6	0.230

Presented as mean ± SD; higher numbers are better. qTOF = quantitative time-of-flight; TOF = time-of-flight.
*Wilcoxon signed-rank tests.

Hemodynamic Data

Figures 4 and 5 show scatter and Bland–Altman plots of component flow velocity and total flow velocity obtained with qTOF and PC. Compared with PC, qTOF demonstrated significant agreement (ICC = 0.89, 95% CI: 0.89–0.89) and significant positive correlation ($r = 0.89$, 95% CI: 0.89–0.89) for component flow velocity, as well as significant agreement (ICC = 0.71, 95% CI: 0.67–0.75) and significant positive correlation ($r = 0.73$, 95% CI: 0.72–0.74) for total flow velocity. Bland Altman 95% limits of agreement between qTOF and PC (qTOF − PC) were (−9.5 cm/s, +9.8 cm/s) for component flow velocity with a bias of 0.1 cm/s, and were (−12.2 cm/s, +9.2 cm/s) for total flow velocity with a mean bias of −1.5 cm/s.

IPSILATERAL VS. CONTRALATERAL HEMODYNAMIC ANALYSIS. qTOF mean total flow velocities were significantly slower in downstream ipsilateral arterial segments than in contralateral arterial segments (12.8 ± 5.0 cm/s vs. 22.0 ± 7.2 cm/s; $P < 0.001$) in 14 patients with unilateral stroke history, ≥50% stenosis, or focal flow alterations (eg, in-stent stenosis, bridged arterial ostia) due to flow diverter placement. Respective ipsilateral and contralateral velocities obtained with PC significantly differed (15.1 ± 3.8 cm/s and 21.5 ± 6.7 cm/s). Arterial flow velocities obtained with qTOF and PC significantly agreed ipsilaterally (ICC = 0.60, 95% CI: 0.12–0.85) and contralaterally (ICC = 0.83, 95% CI: 0.50–0.94).

Discussion

Standard Cartesian head MRA does not provide quantitative hemodynamic data which is predictive of future stroke risk.[5,6] We investigated whether qTOF, a novel multi-echo radial stack-of-stars technique, could be used to simultaneously evaluate the intracranial arteries and quantify intracranial flow without the need for a PC scan. We found that the qTOF method provided excellent image quality that matched or exceeded that of standard Cartesian TOF head MRA, reduced

TABLE 4. Artifact Incidence

	Artifact Count				
	qTOF		TOF		
Artifact Type	n/N	%	n/N	%	*P*-Value*
None	46/72	63.9	27/72	37.5	**0.003**
Susceptibility	25/72	34.7	16/72	22.2	0.140
Motion/Flow	3/72	4.2	31/72	43.1	**<0.001**

qTOF = quantitative time-of-flight; TOF = time-of-flight; n/N = counts/total number of ratings.
*Two-sample test for equality of proportions. Bold indicates statistical significance ($P < 0.05$).

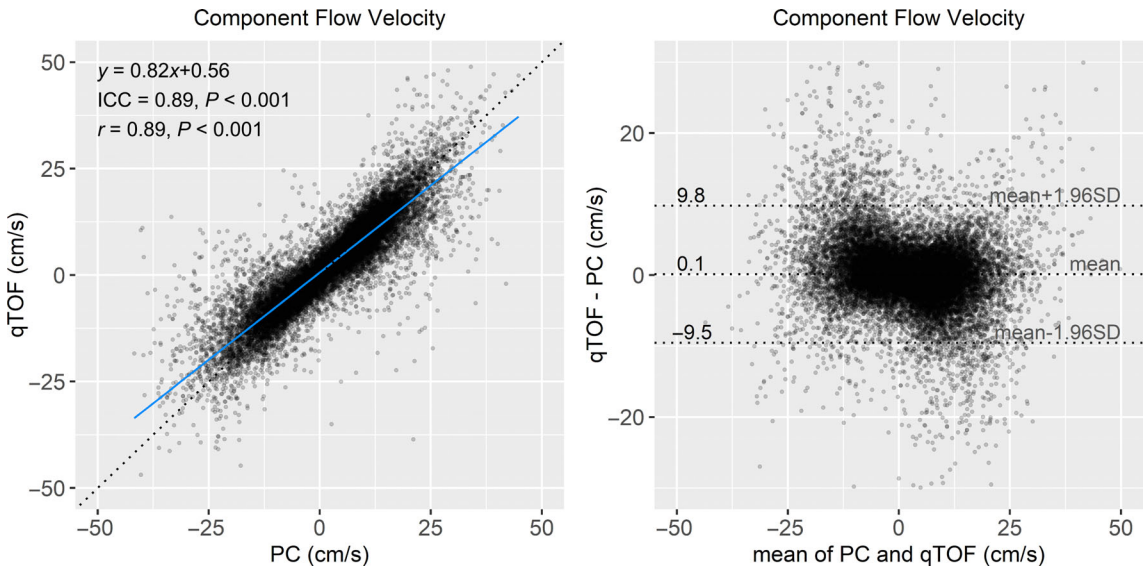

FIGURE 4: Scatter plot (left) and Bland–Altman plot (right) of component flow velocity obtained with qTOF and PC. Component flow velocity measures showed excellent absolute agreement (ICC = 0.89; $P < 0.001$) and small Bland–Altman bias. Blue line is the linear regression line. ICC = intraclass correlation coefficient; qTOF = quantitative time-of-flight; PC = phase contrast.

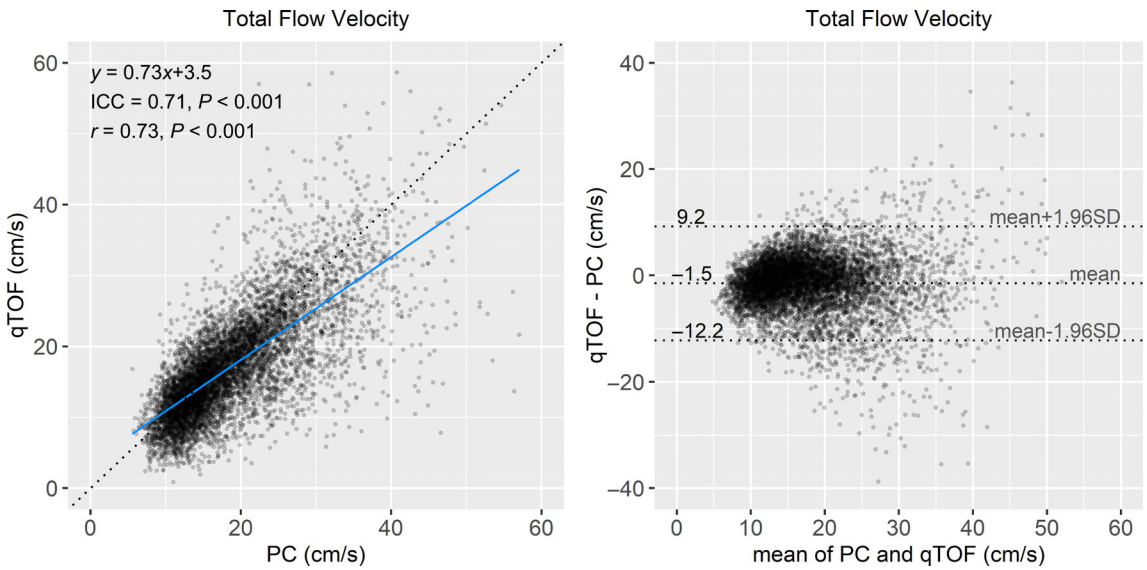

FIGURE 5: Scatter plot (left) and Bland–Altman plot (right) of total flow velocity obtained with qTOF and PC. Total flow velocity measures showed good absolute agreement (ICC = 0.71; $P < 0.001$) and small Bland–Altman bias. Blue line is the linear regression line. ICC = intraclass correlation coefficient; qTOF = quantitative time-of-flight; PC = phase contrast.

the incidence of image artifacts, and provided hemodynamic data that agreed with the well-validated PC approach.

Structural evaluation of the intracranial vessels is essential for detecting arterial pathology such as stenoses, occlusions, and arterial aneurysms. Standard TOF head MRA is a useful non-invasive method for evaluating the structural integrity of the intracranial arteries without the use of contrast agents or ionizing radiation.[12,21,22] However, TOF MRA is sensitive to flow-related artifacts that can distort arterial shape, result in focal signal loss, and obscure evaluation of intracranial arterial pathology.[23] Consequently, improvements to image quality would be desirable. We found that qTOF matched or exceeded the image quality of standard TOF head MRA for evaluating intracranial arterial anatomy and locations of pathology. We ascribe the improved image quality of the qTOF method to the use of a radial-based stack-of-stars data acquisition which is less sensitive to flow artifacts than the standard Cartesian TOF method, and the use of signal subtraction to suppress background signal and improve arterial-to-background contrast.

Differences in image artifact incidence and type were found between qTOF and standard TOF head MRA. qTOF provided a significantly higher proportion of evaluations without artifacts (63.9% vs. 37.5%). In particular,

TOF demonstrated significantly more motion or flow-related artifacts. This observation is consistent with MRI physical expectations as the radial-based qTOF method is less sensitive to motion artifacts.[24] Nonetheless, artifacts were generally mild and image quality was mostly rated as good or excellent with both methods.

Total lesion count varied among the three readers. We suspect this difference is due to human variability in image interpretation, the complex intracranial arterial structure consisting of numerous small and tortuous vessels, the lack of clinical history and context provided to the readers, and the noting of mild lesions that are not usually reported on clinical head MRA exams. Retrospective unblinded review of pathology found by one method and not the other during initial blinded image review found agreement between qTOF and standard TOF in all but a few locations where disease was at most mild.

Image quality scores for qTOF and standard TOF varied among the three readers. In particular, no significant differences between qTOF and TOF were detected in large vessel, small vessel, and overall image quality measures for more-experienced neuroradiologist readers 1 and 2, whereas differences in these measures were significant for less-experienced reader 3. This finding may reflect a possible greater familiarity with the standard TOF image appearance for neuroradiologist readers 1 and 2, or the relatively high level of image quality observed with standard TOF at 3 T than at lower magnetic field strength systems (eg, 1.5 T), that are also routinely interpreted by the same readers.

Intracranial hemodynamics are associated with the risk of future stroke.[5,6,25,26] However, the acquisition of such quantitative hemodynamic data within the intracranial arteries currently requires the use of transcranial Doppler ultrasonography or PC MRA.[9,27] Transcranial Doppler ultrasonography is seldom performed in patients undergoing head MRA due to low availability, high operator dependence, and long examination times (30–60 minutes).[28] On the other hand, the acquisition of PC protocols require additional imaging and time (5–30 minutes) beyond TOF MRA, provide lower spatial resolution than TOF, and consequently are not routinely included in standard head MRA exams.[29–31] In this initial patient study, we found that qTOF provided the same spatial resolution and imaging efficiency (i.e., anatomical coverage per time) of standard TOF head MRA for structural evaluation of the intracranial arteries, while also providing hemodynamic data within every visualized intracranial arterial segment, without requiring any additional scan time. Agreement of total flow velocity with PC was good, whereas agreement of component flow velocity was excellent. Consequently, qTOF shows high potential as an efficient method for simultaneous structural and hemodynamic evaluation of the intracranial arteries that takes no longer than standard head MRA to acquire.

Limitations

This research was performed at a single-center, had a modest sample size, and lacked comparison with invasive digital subtraction angiography (DSA), which is considered the reference standard for structural evaluation of the intracranial arteries. Future work ought to evaluate this approach in a larger patient cohort across multiple institutions, and ideally with DSA correlation. DSA was not acquired in this research study due to patient safety considerations. Contemporaneously acquired computed tomography angiography, which involves the use of iodinated contrast agents and exposure to ionizing radiation, was not available in most subjects involved in this study and thus was not included for comparison. Further work must also establish the long-term and short-term reproducibility of qTOF for both structural hemodynamic evaluation of cerebrovascular disease. The qTOF method evaluated here used signal subtraction to improve arterial-to-background contrast and vessel conspicuity. Further study is needed to determine if un-subtracted source images, which are readily available, may be of added diagnostic utility. Lastly, although outside the scope of the present study, future work should explore deep machine learning strategies[16] to potentially further improve hemodynamic quantitation and agreement with PC.

Conclusion

qTOF provided excellent image quality for evaluating the intracranial arteries and locations of arterial pathology in patients with cerebrovascular disease, matched or exceeded the image quality of standard Cartesian head MRA, reduced the number of studies affected by image artifacts, and yielded quantitative arterial flow velocity data that agreed well with PC. As qTOF shows the potential to match or improve image quality over standard head MRA and simultaneously provide hemodynamic data without requiring any extra imaging time, it represents a promising new approach for efficient structural and hemodynamic evaluation of cerebrovascular disease, as well as for monitoring disease progression and the impact of treatment.

Acknowledgments

This work was supported in part by NIH R01EB027475.

References

1. Roth GA, Mensah GA, Johnson CO. Global Burden of Cardiovascular Diseases and Risk Factors, 1990–2019: Update from the GBD 2019 Study. J Am Coll Cardiol 2020;76:2982-3021.

2. Saini V, Guada L, Yavagal DR. Global epidemiology of stroke and access to acute ischemic stroke interventions. Neurology 2021;97-(20 Suppl 2):S6-S16.

3. Parker DL, Yuan C, Blatter DD. MR angiography by multiple thin slab 3D acquisition. Magn Reson Med 1991;17:434-451.

4. Huston J, Rufenacht DA, Ehman RL, Wiebers DO. Intracranial aneurysms and vascular malformations: Comparison of time-of-flight and phase-contrast MR angiography. Radiology 1991;181:721-730.
5. Amin-Hanjani S, Du X, Zhao M, Walsh K, Malisch TW, Charbel FT. Use of quantitative magnetic resonance angiography to stratify stroke risk in symptomatic vertebrobasilar disease. Stroke 2005;36:1140-1145.
6. Amin-Hanjani S, Pandey DK, Rose-Finnell L, et al. Effect of hemodynamics on stroke risk in symptomatic atherosclerotic vertebrobasilar occlusive disease. JAMA Neurol 2016;73:178-185.
7. Kodoma T, Suzuki Y, Yano T, Watanabe K, Ueda T, Asada K. Phase-contrast MRA in the evaluation of EC-IC bypass patency. Clin Radiol 1995;50:459-465.
8. Wasserman BA, Lin W, Tarr RW, Haacke EM, Müller E. Cerebral arteriovenous malformations: Flow quantitation by means of two-dimensional cardiac-gated phase-contrast MR imaging. Radiology 1995;194: 681-686.
9. Marks MP, Pelc NJ, Ross MR, Enzmann DR. Determination of cerebral blood flow with a phase-contrast cine MR imaging technique: Evaluation of normal subjects and patients with arteriovenous malformations. Radiology 1992;182:467-476.
10. Pernicone JR, Siebert JE, Potchen EJ, Pera A, Dumoulin CL, Souza SP. Three-dimensional phase-contrast MR angiography in the head and neck: Preliminary report. AJR Am J Roentgenol 1990;155:167-176.
11. Huston J, Ehman RL. Comparison of time-of-flight and phase-contrast MR neuroangiographic techniques. Radiographics 1993;13:5-19.
12. Ikawa F, Sumida M, Uozumi T, et al. Comparison of three-dimensional phase-contrast magnetic resonance angiography with three-dimensional time-of-flight magnetic resonance angiography in cerebral aneurysms. Surg Neurol 1994;42:287-292.
13. Huston J, Nichols DA, Luetmer PH, et al. Blinded prospective evaluation of sensitivity of MR angiography to known intracranial aneurysms: Importance of aneurysm size. Am J Neuroradiol 1994;15:1607-1614.
14. Oelerich M, Lentschig MG, Zunker P, Reimer P, Rummeny EJ, Schuierer G. Intracranial vascular stenosis and occlusion: Comparison of 3D time-of-flight and 3D phase-contrast MR angiography. Neuroradiology 1998;40:567-573.
15. Koktzoglou I, Huang R, Edelman RR. Quantitative time-of-flight MR angiography for simultaneous luminal and hemodynamic evaluation of the intracranial arteries. Magn Reson Med 2022;87:150-162.
16. Koktzoglou I, Huang R. Intracranial arterial flow velocity mapping in quantitative time-of-flight MR angiography using deep machine learning. Magn Reson Imaging 2023;100:10-17.
17. Gwet KL. Computing inter-rater reliability and its variance in the presence of high agreement. Br J Math Stat Psychol 2008;61:29-48.
18. Landis JR, Koch GG. The measurement of observer agreement for categorical data. Biometrics 1977;33:159-174.
19. Chan YH. Biostatistics 104: Correlational analysis. Singapore Med J 2003;44:614-619.
20. Cicchetti DV. Guidelines, criteria, and rules of thumb for evaluating normed and standardized assessment instruments in psychology. Psychol Assess 1994;6:284-290.
21. Korogi Y, Takahashi M, Mabuchi N, et al. Intracranial vascular stenosis and occlusion: Diagnostic accuracy of three-dimensional, Fourier transform, time-of-flight MR angiography. Radiology 1994;193:187-193.
22. Willinek WA, Gieseke J, von Falkenhausen M, et al. Sensitivity encoding (SENSE) for high spatial resolution time-of-flight MR angiography of the intracranial arteries at 3.0 T. Rofo 2004;177:21-26.
23. You S-H, Kim B, Yang K-S, Kim BK, Woo S, Park SE. Development and validation of visual grading system for stenosis in intracranial atherosclerotic disease on time-of-flight magnetic resonance angiography. Eur Radiol 2022;32:2781-2790.
24. Glover GH, Pauly JM. Projection reconstruction techniques for reduction of motion effects in MRI. Magn Reson Med 1992;28:275-289.
25. Liebeskind DS, Cotsonis GA, Saver JL, et al. Collaterals dramatically alter stroke risk in intracranial atherosclerosis. Ann Neurol 2011;69: 963-974.
26. Liebeskind DS, Kosinski AS, Lynn MJ, et al. Noninvasive fractional flow on MRA predicts stroke risk of intracranial stenosis. J Neuroimaging 2015;25:87-91.
27. Aaslid R, Markwalder T-M, Nornes H. Noninvasive transcranial Doppler ultrasound recording of flow velocity in basal cerebral arteries. J Neurosurg 1982;57:769-774.
28. van den Wijngaard IR, Holswilder G, van Walderveen MAA, et al. Treatment and imaging of intracranial atherosclerotic stenosis: Current perspectives and future directions. Brain Behav 2016;6:e00536.
29. Zhao M, Amin-Hanjani S, Ruland S, Curcio AP, Ostergren L, Charbel FT. Regional cerebral blood flow using quantitative MR angiography. Am J Neuroradiol 2007;28:1470-1473.
30. Yamashita S, Isoda H, Hirano M, et al. Visualization of hemodynamics in intracranial arteries using time-resolved three-dimensional phase-contrast MRI. J Magn Reson Imaging 2007;25:473-478.
31. Schnell S, Wu C, Ansari SA. Four-dimensional MRI flow examinations in cerebral and extracerebral vessels – Ready for clinical routine? Curr Opin Neurol 2016;29:419-428.